Significance of co-occurring biomarkers in localization of epileptic seizure onset zone

Nawara Mahmood Broti*, Masaki Iwasaki† and Yumie Ono‡
* Electrical Engineering Program, Graduate School of Science and Technology, Meiji University, Japan
E-mail: brotimahmood@gmail.com
† Department of Neurosurgery, National Center Hospital, National Center of Neurology and Psychiatry, Japan
‡ Department of Electronics and Bioinformatics, School of Science and Technology, Meiji University, Japan

***Abstract*— Drug resistant epilepsy (DRE) affects millions of people globally and requires surgical removal of seizure onset zone (SOZ). SOZ localization largely depends on biomarkers such as interictal epileptic discharges (IEDs) and high frequency oscillations (HFOs), though often they are found in both SOZ and non-SOZ areas, causing limited specificity. This study investigates whether temporally co-occurring biomarkers offer better SOZ identification. We analyzed intracranial electrode recordings from 10 DRE patients, evaluating three co-occurrence features: HFO-IED, HFO-HFO, and IED-IED overlaps. Statistical and machine learning analyses confirmed that co-occurrence features have significant difference in distribution within SOZ and non-SOZ region. IED-IED overlap demonstrated robustness in machine learning based classification, achieving the highest accuracy (71.65%), sensitivity (74.08%) and F1 score (0.6727); outperforming both traditional and overlap biomarkers. HFO-IED overlap showed the highest classification specificity (78.81%). These findings highlight the added value of temporal co-occurrence patterns, in enhancing presurgical evaluations for epilepsy treatment.**

I. Introduction

Epilepsy, one of the prevailing neurological diseases, affects a population of 70 million worldwide [1]. One-third of them suffer from drug resistant epilepsy (DRE), in which epileptogenic region or commonly known as seizure onset zone (SOZ) is surgically removed from brain [2]. The surgical outcome of DRE patients largely depends on accurate localization of SOZ during presurgical evaluation. Therefore, doctors rely on clinical and pathological biomarkers of epilepsy to determine SOZ. Interictal epileptic discharges (IEDs) and high frequency oscillations (HFOs) are two widely recognized biomarkers for SOZ detection [3] (Fig. 1).

IEDs are brief bursts of abnormal, spike-like brain activity that occur between seizures and are commonly observed in intracranial EEG (iEEG) recordings of epilepsy patients [4]. IEDs have long served as clinical markers for identifying SOZ. HFOs are faster brain oscillations in the 80-500 Hz range, further classified into ripples (80-250 Hz) and fast ripples (250-500 Hz). Both ictal and interictal HFOs have shown promise in localizing SOZ [5] and predicting surgical outcomes [6]. Signal

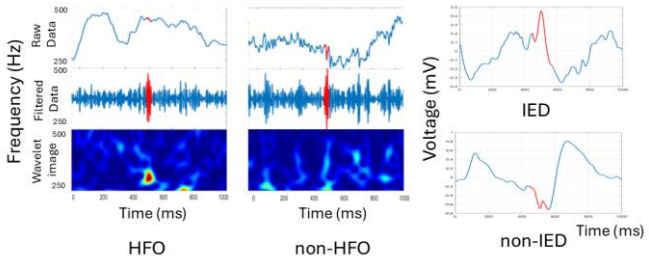

Fig. 1 Examples of HFO signals (left, in red) and IED signals (right, in red) from iEEG data, shown alongside non-HFO and non-IED noise segments.

processing and machine learning have been widely used for automatic SOZ localization from epilepsy biomarkers. Early approaches relied on supervised or unsupervised traditional classifiers with handcrafted features, while recent deep learning methods, including convolutional and residual neural networks, and attention-based networks, enable automated feature extraction and improved identification of epileptic activity [2,3,7,8]. However, both IEDs and HFOs often appear in non-epileptogenic regions as well, limiting their specificity [9]. Differentiating truly pathological biomarkers from benign or protective ones remains a key challenge in epilepsy research.

Recent studies indicate that co-occurring HFOs and IEDs are actively associated with SOZ [10]. Willson et al. reported that the highest functional magnetic resonance imaging (MRI) activation linked to the simultaneous occurrence of HFOs and IEDs tends to be localized within the SOZ [11]. Lachner-Piza et al. found HFO-IEDs more effective than HFOs or IEDs alone in identifying SOZ [12]. Furthermore, some studies have suggested that temporally overlapped HFOs in different electrodes are more likely to be pathological HFOs [13] and that pathological HFOs tend to occur repeatedly in a consistent pattern [14]. This raises the question of how significant the temporal co-occurrence of biomarkers is in identifying the SOZ.

The aim of this study is to determine whether co-occurring biomarkers exhibit different correlations with the SOZ compared non-SOZ, and if so, to quantify these differences and identify the most informative patterns of co-occurrence. We analyzed intracranial electrode recordings from 10 patients and examined the relevance of three co-occurrence scenarios:

1. HFOs and IEDs occurring in the same electrode,

979-8-3315-7206-8/25/$31.00 ©2025 IEEE

2. HFOs co-occurring across different electrodes, and
3. IEDs co-occurring across different electrodes.

Using a combination of statistical analysis and machine learning techniques, we assessed whether accompanying biomarkers improve the accuracy of SOZ identification. The study focused on finding determining if the temporal relationship between HFOs and IEDs could play a critical role in enhancing surgical outcomes.

II. Materials

A. Dataset and Subjects

This study included 10 patients (6 males, 4 females, age 5-62) with focal epilepsy who were evaluated before to surgery at the National Center of Neurology and Psychiatry (NCNP), Tokyo, Japan. Approximately 10 minutes of interictal electroencephalogram (iEEG) recordings were taken over several days, yielding a total data length of 20-120 minutes per subject, primarily using depth electrodes and subdural electrodes. iEEG recordings were obtained using the Nihon Kohden EEG 1200 system. Subdural electrodes consisted of platinum disc electrodes (5 mm diameter, 10 mm inter-electrode spacing), while depth electrodes were platinum cylindrical electrodes (2 mm length, 1.5 mm diameter, 5 mm inter-electrode spacing; Unique Medical Co., Ltd., Tokyo, Japan). The number of electrodes per patient varied between 58 to 98, with sampling rates between 1,000-2,000 Hz. Electrodes located in white matter or outside the brain were eliminated to ensure a focused investigation. NCNP clinicians used three-dimensional MRI, co-registered with postoperative computed tomography scans, to anatomically identify electrode placements. Electrodes from the surgically excised area were labeled SOZ, while the remaining electrodes were classed as non-SOZ. All of the 10 patients achieved seizure freedom following surgery for at least one year. This study was approved by the NCNP and Meiji University Institutional Review Boards (approved number: B2022-049, 22-564).

B. HFO and IED extraction from iEEG signal

IED and HFO segments were extracted from iEEG signals using a bipolar montage. HFO candidates in the fast ripple band (250–500 Hz) were detected from raw iEEG using the RIPPLELAB toolbox [15], applying both the Montreal Neurological Institute [16] and short line length detectors [17]. These segments were then converted into time-frequency images using Morlet wavelet analysis. IED candidates were identified based on Quon et al.'s pipeline [4], which involved filtering and template matching with a spike threshold, followed by conversion into 2D signal images. After finding potential IED and HFO segments, a multi-modal multitask learning (MTL) [18] framework was employed to refine the detection and reduce false positives. A small subset of these IED and HFO images (1500 images each biomarker) was annotated by NCNP epileptologists, which was used to train the MTL model. The model is composed of two parallel convolutional neural network streams, one for HFOs and one for IEDs, connected via cross-stitch units that allowed adaptive feature sharing between tasks [18]. This setup allowed for joint, high-confidence classification of true HFOs and IEDs.

III. Methodology

A. Co- occurrence calculation

Following detection of IEDs and HFOs by the MTL model, we extracted the start times and corresponding electrode name of each IED and HFO events from the raw iEEG signals. To ensure consistency across recordings, all patient data were resampled to a uniform sampling rate of 1000 Hz. We then computed the temporal co-occurrence of events based on start time overlaps within a window of 500, 800, and 1000 milliseconds (ms) across three distinct scenarios (Fig. 2):

(1) HFO and IED co-occurrence within the same electrode,
(2) HFO co-occurrence across different electrodes, and
(3) IED co-occurrence across different electrodes.

For each scenario, we calculated the number of co-occurrence events by counting overlapping start times. This resulted in three co-occurrence features per electrode per patient: HFO-IED, HFO-HFO, and IED-IED. Only the start time of each event was considered, as the duration of HFOs and IEDs varies, and their end times may differ substantially. The typical duration of HFOs ranged from approximately 20–200 ms, whereas IEDs were shorter, lasting about 10–50 ms. A symmetric time window centered on the start time was applied for co-occurrence analysis. When multiple events occurred within the same window, they were counted separately rather than aggregated. In other words, each temporal overlap was considered a single event; thus, when an overlap occurred

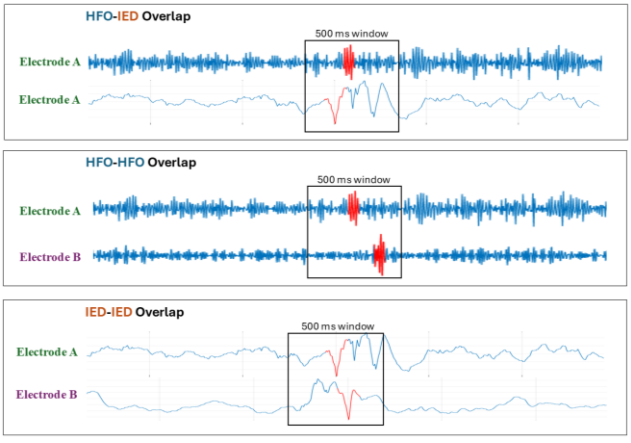

Fig. 2 Examples of co-occurring events in iEEG signals; HFO-IED overlap in the same channel (top); HFO-HFO overlap across different channels (middle); IED-IED overlap across different channels (bottom). Red marks indicate detected events within a 500 ms window.

between two electrodes, both electrodes were assigned one count for that event.

B. Statistical Analysis

The association of each co-occurrence feature (HFO-IED, HFO-HFO, and IED-IED), as well as individual features (IED and HFO population), with SOZ versus non-SOZ electrodes, was evaluated using a statistical analysis pipeline applied across all patients. First, feature values were normalized per patient using z-scoring and then grouped based on electrode labels: SOZ (1) and non-SOZ (0). For each patient, the median value from the SOZ and non-SOZ groups was extracted, resulting in two sets of 10 values- one for each group. The normality of each group's data distribution was assessed using the Shapiro-Wilk test. As the Gaussian distribution was not confirmed, particularly within the SOZ groups, non-parametric statistical tests were employed for subsequent analyses. Statistical significance of the differences between these paired groups was then assessed using the non-parametric Wilcoxon signed-rank test. A p-value less than 0.05 ($p < 0.05$) in the Wilcoxon signed-rank test indicated a statistically significant difference between the SOZ and non-SOZ groups (hypothesis = 1); while p-value ≥ 0.05 indicated no significant difference (hypothesis = 0). To visualize group differences, we plotted the mean z-scored feature of all patients' distributions for SOZ and non-SOZ groups using violin plots.

C. Validation using Machine learning

To evaluate how well each co-occurrence feature (HFO-IED, HFO-HFO, IED-IED overlap) could classify SOZ versus non-SOZ electrodes, we employed a RUSBoost (Random Under-Sampling Boosting) [19] ensemble classifier with a leave-one-patient-out (LOPO) cross-validation scheme. Each electrode was represented by a single feature value per feature. We specifically chose RUSBoost classifier as it is designed to handle imbalanced classification problems, where one class (SOZ electrodes) has far fewer samples than the other (non-SOZ). Each patient's data was normalized through z-scoring. In each of the 10 LOPO folds, the classifier was trained on data from 9 patients and tested on the remaining held-out patient. The RUSBoost model consisted of 50 shallow decision trees (each with max 5 splits) with no additional hyperparameter tuning performed. Parameters, such as the learning rate and sampling ratio for random under-sampling, were left at MATLAB default values. This procedure was repeated separately for each co-occurrence feature. For each fold, we computed classification metrics- accuracy, sensitivity, specificity, and F1-score- based on the predicted labels of the test patient's electrodes. These metrics were then averaged across all folds to evaluate overall model performance. Additionally, we calculated the standard error (SE) across the 10 patient-level metrics following Equation 1.

$$SE = \frac{\sigma}{\sqrt{n}} \quad (1)$$

Where σ is the standard deviation of the metric across patients and n is total number of patients (n=10). To establish baseline performance, the same LOPO classification was performed using only the IED population feature and only the HFO population feature. Finally, to determine which feature provided the best discrimination between SOZ and non-SOZ electrodes, we compared the performance metrics of each co-occurrence feature against each other and against the individual IED and HFO population features across folds.

IV. Results

Ten patients who achieved seizure freedom (to this date) were included in the statistical and machine learning analysis. Table I presents the p-values obtained from paired Wilcoxon signed-rank tests for each co-occurrence feature and base feature across three temporal overlap windows: 500 ms, 800 ms, and 1000 ms. The results show that all features demonstrated statistically significant differences between SOZ and non-SOZ groups ($p < 0.05$), indicating rejection of the null hypothesis. Although all features reached significance, there were notable differences in the p-values across features and window sizes. In the signed-rank test, IED-IED overlap, HFO-HFO overlap, and the IED population all reached the lowest observed p-value ($p = 0.00195$), reinforcing their robustness. Among them, IED-IED overlap consistently yielded the lowest p-values in all windows, highlighting its strong discriminative power.

In the case of HFO-IED overlap, a decreasing trend in p-values was observed as the time window increased, suggesting that larger temporal windows may more effectively capture the dynamics of multiple biomarker co-occurrence. Conversely, for the HFO-HFO feature, an opposite pattern was noted, with the p-value slightly increasing in the 1000 ms window compared to the 500 ms and 800 ms windows. Overall, IED-IED overlap emerged as the most robust and consistent feature, showing high statistical significance across both tests and all window sizes. HFO-HFO and HFO-IED overlaps also demonstrated meaningful group differences, particularly with longer windows, though they were slightly less consistent at shorter durations.

Table I P-values from paired Wilcoxon signed-rank test comparing feature values between SOZ and non-SOZ electrodes

Time Window	HFO-IED	HFO-HFO	IED-IED	HFO	IED
500 ms	0.03125	0.00195	0.00195	0.00586	0.00195
800 ms	0.03125	0.00195	0.00195		
1000 ms	0.01563	0.00391	0.00195		

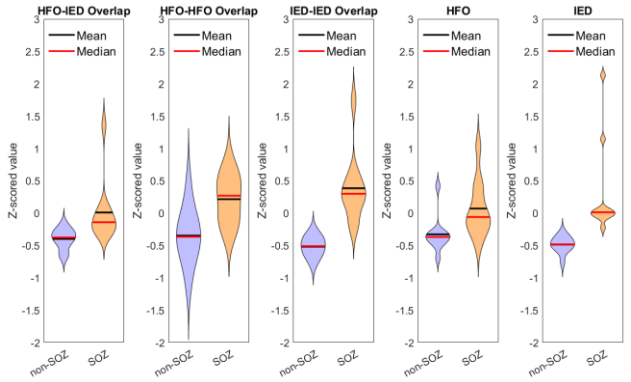

Fig. 3 Violin plots show higher mean and median overlap in SOZ electrodes across all features. Distributions for SOZ are more widely spread, especially for HFO-IED and IED-IED overlap feature as well as IED population feature, indicating stronger clustering. HFO–HFO overlap shows a wide but low distribution, reflecting comparatively weak difference between SOZ and non-SOZ groups.

For further statistical comparison, the 1000 ms window overlap data was selected as it yielded good statistical significance scores in most cases. For each feature. we normalized each patient's data by computing z-score and grouped all patient data together into SOZ and non-SOZ electrode categories. Fig. 3 shows violin plots using mean z-scored feature distributions for non-SOZ and SOZ groups, respectively. Notably, IED-IED overlap and IED population show strong, consistent, and separated distributions, making them the most robust features. In the HFO-IED plot, the SOZ distribution shows a moderately wider spread and higher mean and median value with some extreme outliers in the SOZ region compared to the non-SOZ region. The HFO-HFO plot reveals very high mean and median values in the SOZ group; however, the distribution was comparable between SOZ and non-SOZ regions.

Table II presents the average performance metrics along with their SE across 10 patients (indicated as ±) from the LOPO cross-validation experiment, reported separately for each co-occurrence feature as well as for the individual IED and HFO population features. Among the evaluated metrics, the IED-IED overlap feature achieved the highest accuracy ($71.4 \pm 3.35\%$) and sensitivity ($74.08 \pm 6.44\%$), along with the smallest SE. It also yielded the highest F1-score (0.6727 ± 0.033), with the second lowest variability across patients, highlighting its strong and balanced classification performance. The IED-IED overlap marginally improves upon the baseline IED feature across all metrics. The lower SE suggests consistent performance across patients, which can be valuable in clinical contexts. Notably, the HFO-IED overlap achieved the highest specificity ($78.81 \pm 2.53\%$), followed by the IED-IED overlap with $74.10 \pm 3.98\%$ sensitivity. HFO-IED overlap consistently outperforms the HFO baseline across all metrics, and the IED baseline in accuracy and specificity. This suggests that co-occurrence with IEDs enhances the discriminative power of HFOs. However, in terms of sensitivity, the HFO-IED co-occurrence feature demonstrated a comparatively lower value than the IED baseline, along with greater variability across patients, indicating a limitation in its generalizability. Although HFO-HFO outperformed the HFO baseline across all metrics, its overall performance remained lower than the other co-occurrence features. Nonetheless, the modest SE value indicates stability across patients. Notably, it achieved a 6.45% improvement in accuracy over the HFO feature. These results highlight the potential of co-occurrence features in enhancing SOZ classification.

Table II SOZ and non-SOZ classification performance

	HFO-IED	**HFO-HFO**	**IED-IED**	**HFO**	**IED**
Accuracy	69.87 ±4.98%	61.04 ±2.41%	71.45 ±3.35%	54.59 ±3.79%	69.17 ±3.70%
Sensitivity	65.71 ±8.46%	56.75 ±7.00%	74.08 ±6.44%	48.20 ±8.67%	70.17 ±7.09%
Specificity	78.81 ±2.53%	69.84 ±4.44%	74.10 ±3.98%	66.47 ±5.17%	71.68 ±3.88%
F1 score	0.6360 ±0.074	0.6034 ±0.030	0.6727 ±0.033	0.5408 ±0.067	0.6516 ±0.036

V. Discussion

This study highlights the potential of co-occurring biomarkers as informative features for SOZ localization in focal epilepsy. Findings demonstrate that co-occurrence features can outperform traditional biomarkers (i.e., HFO or IED rates alone) in differentiating SOZ from non-SOZ electrodes. Statistical analysis revealed that simultaneously occurring IED spikes in different electrodes were the most robust feature, showing significant differences between SOZ and non-SOZ electrodes. The IED-IED overlap also achieved the best accuracy and F1 score in machine learning classification, compared to other types of overlap features as well as IED and HFO population features. The co-occurrence of HFO and IED within the same electrode yielded strong classification performance as a machine learning feature, achieving the highest specificity and demonstrating its effectiveness in accurately identifying non-SOZ electrodes. The high specificity likely stems from its clear separation between SOZ and non-SOZ, low variability in non-SOZ, and strong link to pathological activity, making HFO-IED overlap a reliable marker for identifying non-SOZ electrodes. HFO-HFO overlap also showed discriminative power with statistical significance between SOZ and non-SOZ groups; however, its classification performance was comparatively weaker. The poor classification performance may be due to the physiological and widespread occurrence of HFOs in both SOZ

and non-SOZ regions, also noticed in the violin plot, thus creating high variability and limiting its effectiveness as a discriminative feature for machine learning classification.

Interictal spikes such as IEDs reflect abnormal hypersynchrony of neurons at the large-scale network level, while high-frequency abnormality such as HFOs occur at smaller-scale networks. These events can happen independently, but their co-occurrence indicates hyperexcitability across multiple network scales, making it a stronger marker of abnormal activity. Previous studies have implied that co-occurring HFOs and IEDs are closely associated with SOZ and temporally overlapping HFOs across different electrodes are more likely to represent pathological activity [10-14]. Our results validate these findings and add that overlapping IEDs can also be considered a potential marker of pathological activity.

This study has few limitations to consider. First, the resected brain regions may encompass both true SOZ and surrounding healthy tissue, which could result in some healthy region electrodes being labeled as SOZ, potentially contributing to false-negative classifications. Furthermore, the IEDs and HFOs were extracted using an MTL model instead of expert annotation. While the model offers time efficiency and has shown high confidence in detecting biomarkers, it limits the amount of usable data, and the correctness of the selected events cannot be fully verified. Moreover, the relatively small patient population restricts the generalizability of the findings. Future work will focus on expanding the good outcome patient cohorts, proper validation of selected biomarkers from experts and comparison between several epilepsy biomarkers.

VI. Conclusions

In this study, we explored the effectiveness of co-occurrence features, such as HFO-IED, HFO-HFO, and IED-IED overlaps, in localizing the SOZ in focal epilepsy patients. Our results showed that co-occurrence features, particularly IED-IED and HFO-IED overlap, outperformed individual biomarker rates in both statistical analysis and machine learning based classification tasks. These features captured important temporal relationships between events, offering a more accurate reflection of epileptogenic activity. Expanding the dataset and comparing a wider range of biomarkers could further improve the precision of SOZ localization and ultimately enhance surgical success rates.

VII. Acknowledgment

We acknowledge Masaki Sawada for his contribution in data processing. We also acknowledge the contribution of National Center of Neurology and Psychiatry, Tokyo, Japan for assistance in data collection and annotation. This study was supported by JSPS KAKENHI (22K09296 and 25K12401).

References

[1] R. D. Thijs, R. Surges, T. J. O'Brien, and J. W. Sander, 'Epilepsy in adults', Lancet, vol. 393, no. 10172, pp. 689–701, 2019.

[2] N. M. Broti, M. Iwasaki, and Y. Ono, 'Machine learning detection of epileptic seizure onset zone from iEEG', Biomed. Eng. Lett., 2025.

[3] M. R. Islam, X. Zhao, Y. Miao, H. Sugano, and T. Tanaka, 'Epileptic sei zure focus detection from interictal electroencephalogram: a sur vey', Cogn Neurodyn, vol. 17, no. 1, pp. 1–23, 2023.

[4] R. J. Quon et al., 'AiED: Artificial intelligence for the detection of intracranial interictal epileptiform discharges', Clinical neurophysiology, vol. 133, pp. 1–8, 2022.

[5] N. M. Broti, M. Sawada, Y. Takayama, K. Iijima, M. Iwasaki, and Y. Ono, 'Automated detection of interictal High-frequency oscillations for epileptogenic zone localization', Adv Biomedical Eng, vol. 13, pp. 100–107, 2024.

[6] V. Dimakopoulos et al, Protocol for multicentre comparison of interictal high-frequency oscillations as a predictor of seizure freedom', Brain Commun., vol. 4, no. 3, p. fcac151, 2022.

[7] A. F. Hussein et al., 'Focal and non-focal epilepsy localization: A review', IEEE Access, vol. 6, pp. 49306–49324, 2018.

[8] S. S. Balaji and K. K. Parhi, 'Seizure onset zone identification from iEEG: A review', IEEE Access, vol. 10, pp. 62535–62547, 2022.

[9] T. A. Guth et al., 'Interictal spikes with and without high-frequency oscillation have different single-neuron correlates', Brain, vol. 144, no. 10, pp. 3078–3088, 2021.T. A. Guth et al., 'Interictal spikes with and without high-frequency oscillation have different single-neuron correlates', Brain, vol. 144, no. 10, pp. 3078–3088, 2021.

[10] A. H. Mooij, G. J. M. Huiskamp, E. Aarts, C. H. Ferrier, K. P. J. Braun, and M. Zijlmans, 'Accurate differentiation between physiological and pathological ripples recorded with scalp-EEG', Clin. Neurophysiol., vol. 143, pp. 172–181, 2022.

[11] W. Wilson et al., 'The hemodynamic response to co-occurring interictal epileptiform discharges and high-frequency oscillations localizes the seizure-onset zone', Epilepsia, vol. 65, no. 9, pp. 2764–2776, 2024.

[12] D. Lachner-Piza, J. Jacobs, J. C. Bruder, A. Schulze-Bonhage, T. Stieglitz, and M. Du Mpelmann, 'Automatic detection of high-frequency oscillations and their sub-groups co-occurring with interictal epileptic- spikes', J Neural Eng, vol. 17, no. 1, 2020.

[13] L. A. Ewell, K. B. Fischer, C. Leibold, S. Leutgeb, and J. K. Leutgeb, 'The impact of pathological high-frequency oscillations on hippocampal network activity in rats with chronic epilepsy', Elife, vol. 8, 2019.

[14] S. Liu et al., 'Stereotyped high-frequency oscillations discriminate seizure onset zones and critical functional cortex in focal epilepsy', Brain, vol. 141, no. 3, pp. 713–730, 2018.

[15] M. Navarrete, C. Alvarado-Rojas, M. Le Van Quyen, and M. Valderrama, 'RIPPLELAB: A comprehensive application for the detection, analysis and classification of high frequency oscillations in electroencephalographic signals', PloS one, vol. 11, no. 6, 2016.

[16] R. Zelmann, F. Mari, J. Jacobs, M. Zijlmans, F. Dubeau, and J. Gotman, 'A comparison between detectors of high frequency oscillations', Clin. Neurophysiol., vol. 123, no. 1, pp. 106–116, 2012.

[17] A. B. Gardner, G. A. Worrell, E. Marsh, D. Dlugos, and B. Litt, 'Human and automated detection of high-frequency oscillations in clinical intracranial EEG recordings', Clinical neurophysiology, vol. 118, no. 5, pp. 1134–1143, 2007.

[18] N. M. Broti, M. Sawada, Y. Takayama, K. Iijima, M. Iwasaki, and Y. Ono, 'Multi-modal Multitask Learning Model for Simultaneous Classification of Two Epilepsy Biomarkers', International Conference on Pattern Recognition, pp. 235–250, 2025.

[19] C. Seiffert, T. M. Khoshgoftaar, J. Van Hulse, and A. Napolitano, 'RUSBoost: A hybrid approach to alleviating class imbalance', IEEE Trans. Syst. Man Cybern. A Syst. Hum., vol. 40, no. 1, pp. 185–197, 2010.